Supporting information for

Anodic activity of hydrated and anhydrous Iron (II) oxalate in Li-ion batteries

Fatemeh Keshavarz,[1] Marius Kadek,[2,3] Bernardo Barbiellini[1,3] and Arun Bansil[3]

[1]Department of Physics, School of Engineering Science, LUT University, FI-53851 Lappeenranta, Finland; Fatemeh.Keshavartz@lut.fi, Bernardo.Barbiellini@lut.fi

[2]Hylleraas Centre for Quantum Molecular Sciences, UiT The Arctic University of Norway, N-9037 Tromsø, Norway; Marius.Kadek@uit.no

[3]Department of Physics, Northeastern University, Boston, Massachusetts 02115, USA; Ar.Bansil@northeastern.edu
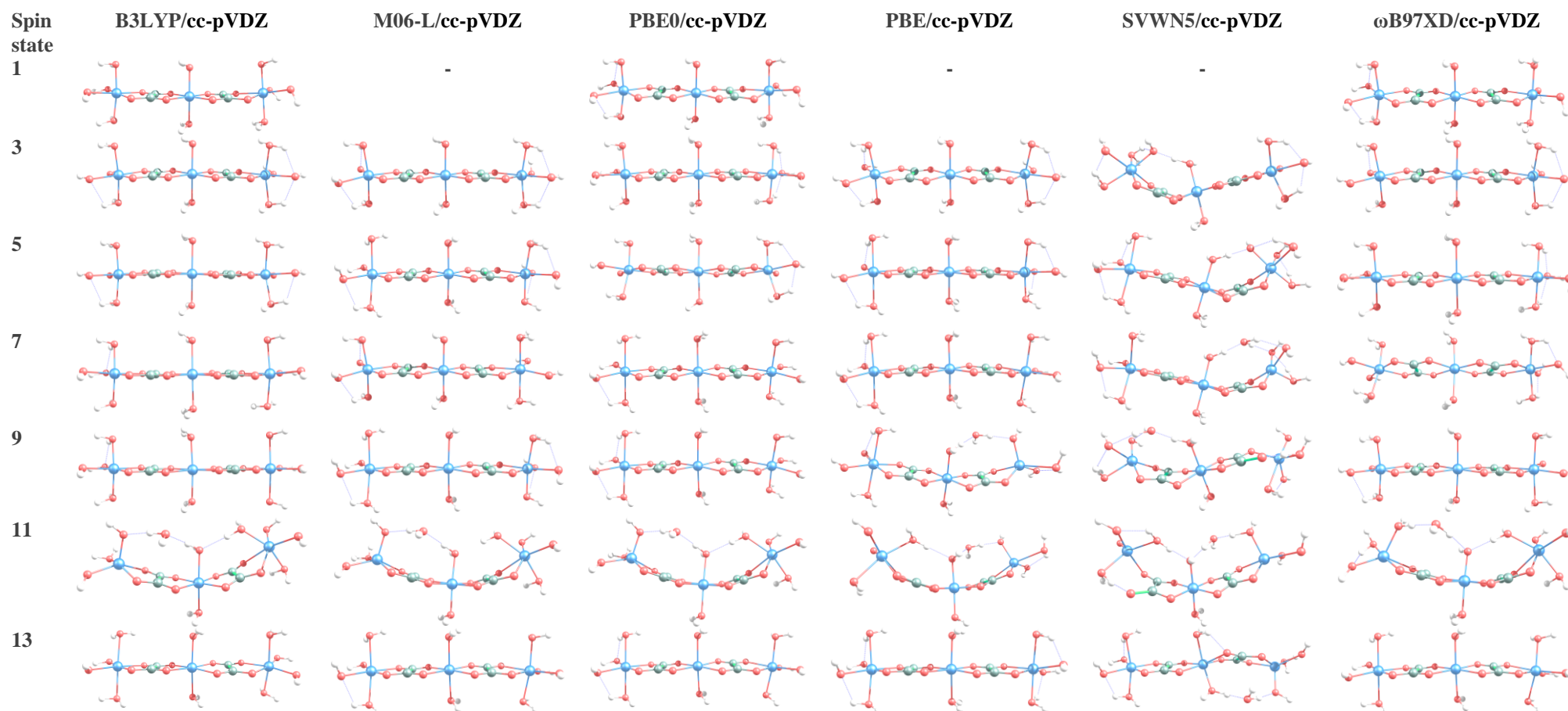
Figure S1. Geometry of FOD optimized for different spin states at various computational levels. The blue, red, grey, and white spheres represent the Fe, oxygen, carbon, and hydrogen atoms, respectively.

Table S1. Zero-point energy corrected electronic energy (E), Gibbs free energy (G; 298.15 K and 1 atm) and the total spin of FOD before (S^2) and after (S^2A) annihilation in different spin states for various computational levels. [a]

Spin state	B3LYP/cc-pVDZ	M06-L/cc-pVDZ	PBE0/cc-pVDZ	PBE/cc-pVDZ	SVWN5/cc-pVDZ	ωB97XD/cc-pVDZ
1	*G*: -5307.658849	*G*: -	*G*: -5305.238971	*G*: -	*G*: -	*G*: -5307.043445
	E: -5307.591235	*E*: -	*E*: -5305.173962	*E*: -	*E*: -	*E*: -5306.977308
	s2: -	*s2*: -	*s2*: -	*s2*: -	*s2*: -	*s2*: -
	s2A: -	*s2A*: -	*s2A*: -	*s2A*: -	*s2A*: -	*s2A*: -
3	*G*: -5307.753568	*G*: -5307.375185	*G*: -5305.360495	*G*: -5305.426232	*G*: -5289.459114	*G*: -5307.198915
	E: -5307.685141	*E*: -5307.308634	*E*: -5305.292187	*E*: -5305.358306	*E*: -5289.397964	*E*: -5307.131639
	s2: 3.243904	*s2*: 2.422780	*s2*: 3.891242	*s2*: 2.897529	*s2*: 2.023308	*s2*: 2.91406
	s2A: 3.209425	*s2A*: 2.065606	*s2A*: 5.396047	*s2A*: 2.460702	*s2A*: 2.000317	*s2A*: 2.597536
5	*G*: -5307.761796	*G*: -5307.402221	*G*: -5305.370724	*G*: -5305.444818	*G*: -5289.457101	*G*: -5307.207484
	E: -5307.689493	*E*: -5307.332308	*E*: -5305.299414	*E*: -5305.374473	*E*: -5289.393556	*E*: -5307.137932
	s2: 6.740685	*s2*: 6.460798	*s2*: 7.218195	*s2*: 6.402992	*s2*: 6.047686	*s2*: 6.548532
	s2A: 6.185071	*s2A*: 6.054771	*s2A*: 6.603131	*s2A*: 6.032645	*s2A*: 6.000732	*s2A*: 6.097592
7	*G*: -5307.791662	*G*: -5307.436160	*G*: -5305.397885	*G*: -5305.464215	*G*: -5289.450097	*G*: -5307.250513
	E: -5307.715492	*E*: -5307.363363	*E*: -5305.323984	*E*: -5305.388543	*E*: -5289.383851	*E*: -5307.178164
	s2: 12.415455	*s2*: 12.371319	*s2*: 12.825456	*s2*: 12.38804	*s2*: 12.114234	*s2*: 12.118377
	s2A: 12.033226	*s2A*: 12.016256	*s2A*: 12.137185	*s2A*: 12.017738	*s2A*: 12.002951	*s2A*: 12.001842
9	*G*: -5307.826438	*G*: -5307.450032	*G*: -5305.440490	*G*: -5305.489168	*G*: -5289.460479	*G*: -5307.198855
	E: -5307.750725	*E*: -5307.375549	*E*: -5305.365555	*E*: -5305.417012	*E*: -5289.392120	*E*: -5307.160526
	s2: 20.183703	*s2*: 20.104593	*s2*: 20.414764	*s2*: 20.090569	*s2*: 20.074218	*s2*: 20.133789
	s2A: 20.003767	*s2A*: 20.00182	*s2A*: 20.011522	*s2A*: 20.001541	*s2A*: 20.000877	*s2A*: 20.002271
11	*G*: -5307.849471	*G*: -5307.496262	*G*: -5305.471087	*G*: **-5305.494913**	*G*: -5289.482608	*G*: -5307.295506
	E: -5307.776272	*E*: -5307.425109	*E*: -5305.398796	*E*: **-5305.422536**	*E*: -5289.413401	*E*: -5307.223970
	s2: 30.780760	*s2*: 30.041531	*s2*: 31.110211	*s2*: 30.075807	*s2*: 30.057197	*s2*: 30.052458
	s2A: 30.050103	*s2A*: 30.000255	*s2A*: 30.131397	*s2A*: 30.000699	*s2A*: 30.000344	*s2A*: 30.000355
13	*G*: **-5307.858666**	*G*: **-5307.505173**	*G*: **-5305.488488**	*G*: -5305.494675	*G*: -5289.469053	*G*: **-5307.306642**
	E: **-5307.778597**	*E*: **-5307.425488**	*E*: **-5305.408078**	*E*: -5305.415639	*E*: -5289.396779	*E*: **-5307.228653**
	s2: 42.055523	*s2*: 42.098075	*s2*: 42.064075	*s2*: 42.065012	*s2*: 42.108891	*s2*: 42.048678
	s2A: 42.000288	*s2A*: 42.001023	*s2A*: 42.000341	*s2A*: 42.000504	*s2A*: 42.001334	*s2A*: 42.000233

[a] The ground spin state and structures with spin contamination, imaginary frequencies and structural irregularities are distinguished by bolded, orange, italic and red values, respectively.

Section S1. Computational level validation

Geometry of the FOD model optimized for the ground spin-state (13tet) at various computational levels is compared with the available experimental data in Table S2. PBE0/cc-pVDZ is seen to be the optimal method with the smallest error in prediction of the unit-cell geometry of FOD. Beyond PBE0/cc-pVDZ , B3LYP/cc-pVDZ, followed by ωB97XD/cc-pVDZ and PBE/cc-pVDZ), yield reasonable geometries.

Table S2. Comparison of the geometry of the FOD model (13tet) optimized at different levels of theory with the experimental structure. [a]

Level	Fe-Oo (Å)	Fe-Ow (Å)	Ow-H (Å)	H-Ow-H (°)	C-Oo (Å)	Oo-C-C (°)	Oox-C-Ox (°)	Ow-Fe-Ow (°)	MAE (%)
Exp.[b]	2.14	2.11	0.96	104.0	1.25	116.6	126.8	170-182	
B3LYP/cc-pVDZ	2.12	2.22	0.97	105.4	1.26	117.0	127.0	176.7	2.72
M06L/cc-pVDZ	2.10	2.23	0.97	104.5	1.26	117.2	127.1	174.5	3.49
PBE0/cc-pVDZ	2.11	2.21	0.97	105.4	1.25	117.1	127.0	176.9	2.61
PBE/cc-pVDZ	2.08	2.24	0.98	104.0	1.27	117.2	126.6	174.4	3.22
ωB97XD/cc-pVDZ	2.12	2.22	0.97	104.0	1.25	117.1	127.1	177.5	3.09
PBE0/6-31+G*	2.10	2.20	0.97	106.8	1.25	117.0	127.2	178.6	4.13
PBE0/6-311++G**	2.11	2.20	0.96	107.6	1.24	117.0	127.4	179.4	5.47
PBE0/def2-TZVP	2.10	2.22	0.96	107.2	1.24	117.2	127.1	178.5	3.64

[a] Theoretical values are average bond lengths and angles referring to the central Fe^{2+} ion. The water and oxalate oxygen atoms are distinguished as Ow and Oo, respectively. MAE: mean absolute error.
[b] The Ow-Fe-Ow bond angle range is adopted from Müller et al. [1]. All other experimental data are taken from Echigo and Kimaka [2].

Next, the band gap between the highest occupied (HOMO) and lowest unoccupied (LUMO) molecular orbitals of FOD were compared with the experimentally estimated band gaps. The band gaps predicted at the PBE0/cc-pVDZ, B3LYP/cc-pVDZ, ωB97XD/cc-pVDZ and PBE/cc-pVDZ levels are 4.94 eV, 4.42 eV, 8.77 eV and 1.36 eV, respectively. The experimentally reported band gaps are 2.10 eV [3] and 2.17 eV [4], which are closest to the PBE/cc-pVDZ values. Substantial errors in the calculated band gaps partly result from the choice of a small model rather than a periodic structure.

Finally, the harmonic vibrational frequencies of the FOD model calculated at the PBE0/cc-pVDZ level are in reasonable accord with the values obtained for the most distinct vibrational modes from the FT-IR spectra [1] (given in parentheses) as follows:

O-H stretching: 3801 cm^{-1} (vs. 3311 cm^{-1}); antisymmetric O-C-O stretching: 1518 cm^{-1} (vs. 1605 cm^{-1}); symmetric elongation of the O-C-O bonds: 1388 and 1378 cm^{-1} (vs. 1361 and 1313 cm^{-1}); C=C bond vibrations: 867 cm^{-1} (vs. 822 cm^{-1}); and Fe-O bond stretching: 456 cm^{-1} (vs. 482 cm^{-1}).

Bearing these results in mind, we chose PBE0/cc-pVDZ as the optimal level for further computations. However, selected calculations were also performed at the B3LYP/cc-pVDZ, ωB97XD/cc-pVDZ and PBE/cc-pVDZ levels. Particularly, the electronic band structure calculations for the periodic unit cell were performed at the PBE/ucc-pVDZ level.
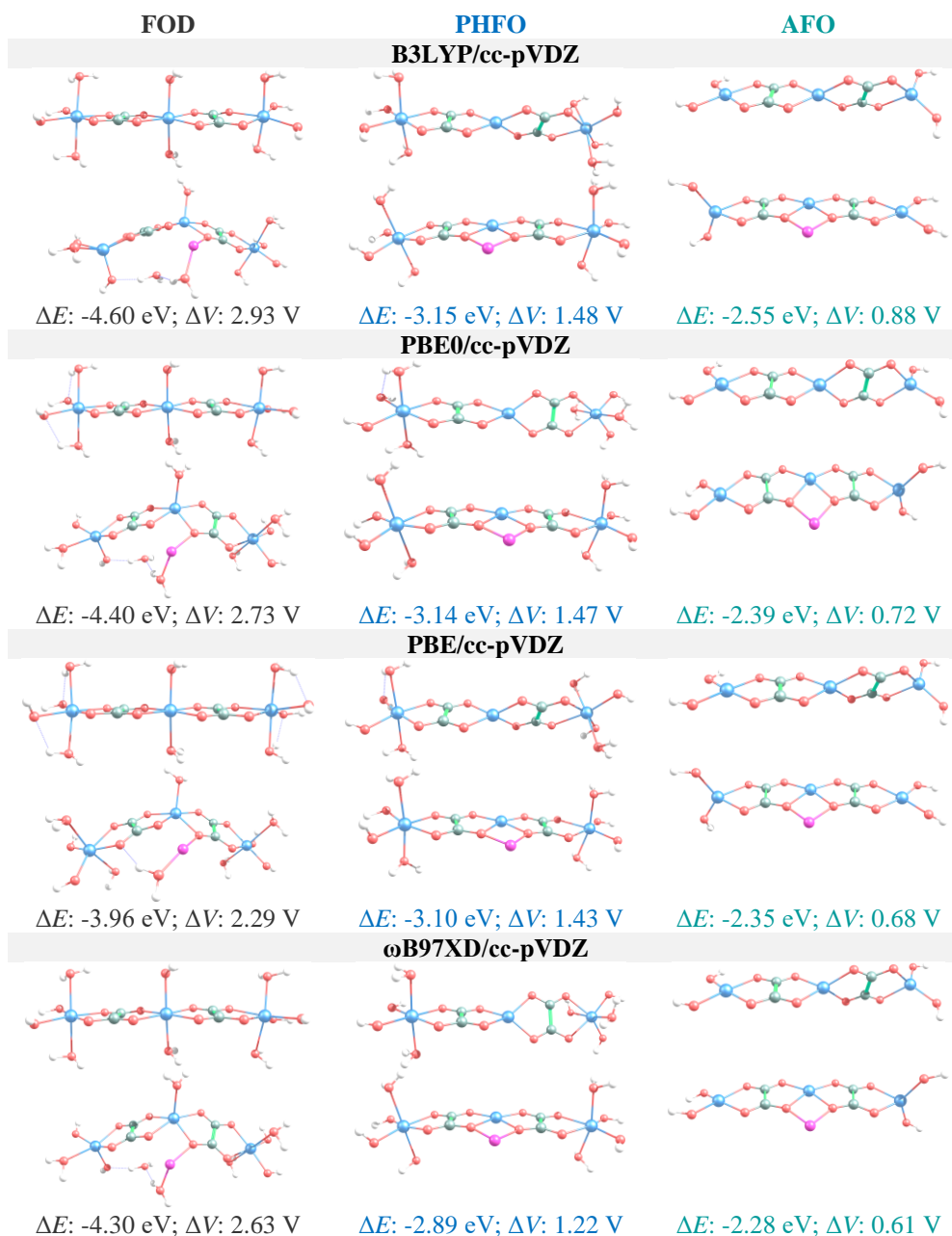
FOD	PHFO	AFO
B3LYP/cc-pVDZ		

ΔE: -4.60 eV; ΔV: 2.93 V	ΔE: -3.15 eV; ΔV: 1.48 V	ΔE: -2.55 eV; ΔV: 0.88 V
PBE0/cc-pVDZ		

ΔE: -4.40 eV; ΔV: 2.73 V	ΔE: -3.14 eV; ΔV: 1.47 V	ΔE: -2.39 eV; ΔV: 0.72 V
PBE/cc-pVDZ		

ΔE: -3.96 eV; ΔV: 2.29 V	ΔE: -3.10 eV; ΔV: 1.43 V	ΔE: -2.35 eV; ΔV: 0.68 V
ωB97XD/cc-pVDZ		

ΔE: -4.30 eV; ΔV: 2.63 V	ΔE: -2.89 eV; ΔV: 1.22 V	ΔE: -2.28 eV; ΔV: 0.61 V

Figure S2. Changes in the structure of FOD, PHFO and AFO upon Li^+ intercalation and the corresponding adsorption energies (zero-point energy corrected; ΔE) and open circuit voltages with respect to Li cathode (ΔV), at different levels of theory. All properties are reported at the 13tet ground spin state. The upper (lower) row structures are the structures optimized in the absence (presence) of Li^+. The pink, blue, red, grey, and white spheres represent Li, Fe, oxygen, carbon and hydrogen atoms, respectively.
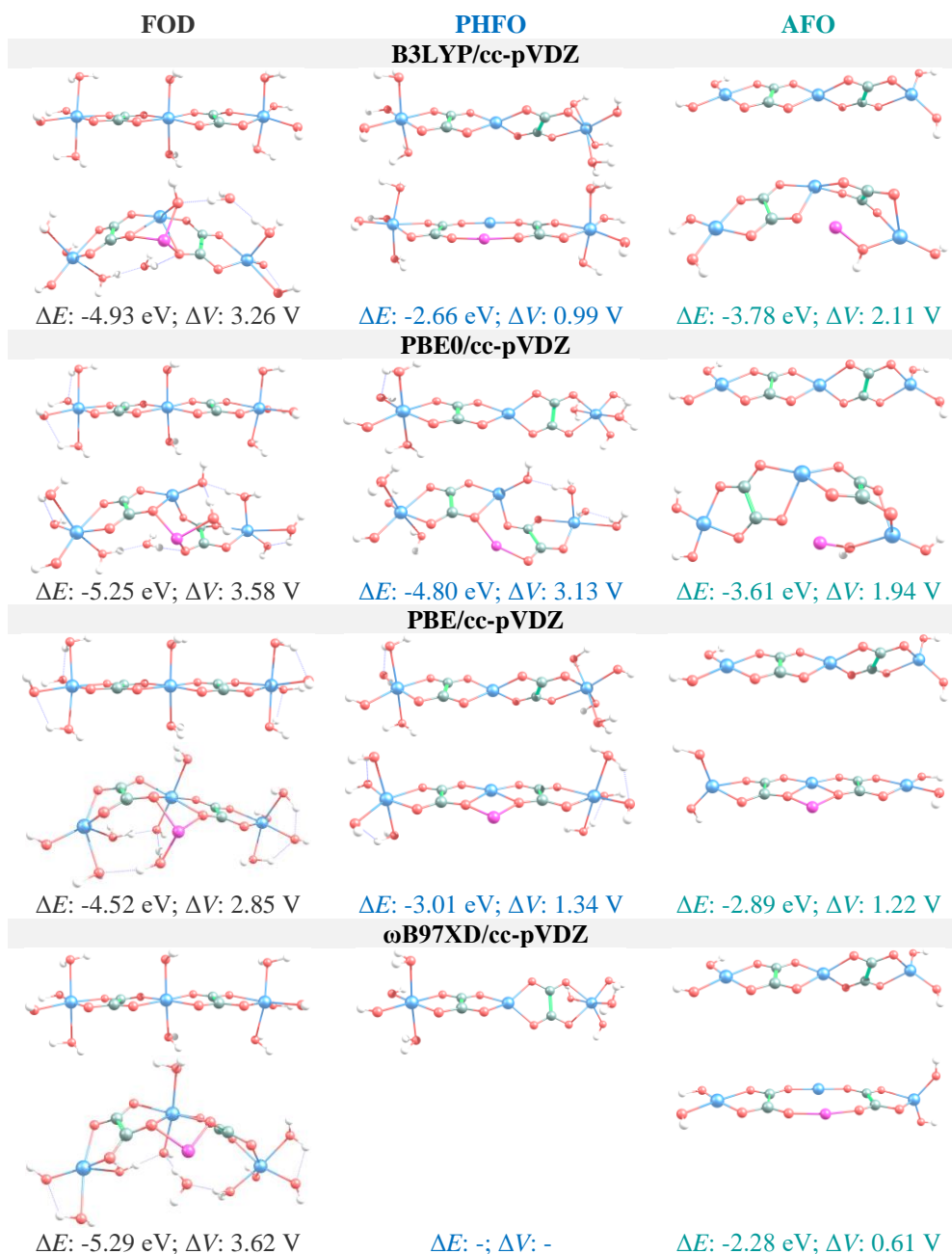
Figure S3. Changes in the structure of FOD, PHFO and AFO upon Li^0 intercalation and the corresponding adsorption energies (zero-point energy corrected; ΔE) and open circuit voltages with respect to Li cathode (ΔV), at various levels of theory. Properties of the Li^0 containing FOD, PHFO and AFO models are given at their 14tet, 14tet and 12tet ground spin-states, respectively. The upper (lower) row structures are the structures optimized in the absence (presence) of Li^0. The pink, blue, red, grey, and white spheres represent the Li, Fe, oxygen, carbon and hydrogen atoms, respectively.
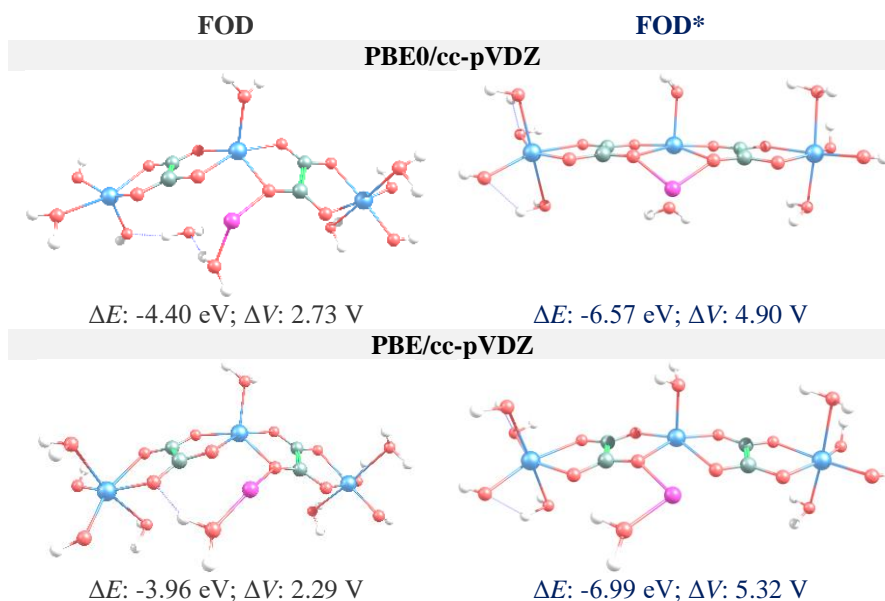
	FOD	FOD*
PBE0/cc-pVDZ		
ΔE: -4.40 eV; ΔV: 2.73 V		ΔE: -6.57 eV; ΔV: 4.90 V
PBE/cc-pVDZ		
ΔE: -3.96 eV; ΔV: 2.29 V		ΔE: -6.99 eV; ΔV: 5.32 V

Figure S4. The structure of FOD after Li^+ intercalation and the corresponding adsorption energy (zero-point energy corrected; ΔE) and the open-circuit voltage with respect to Li cathode (ΔV), at the PBE0/cc-pVDZ and PBE/cc-pVDZ levels. The pink, blue, red, grey, and white spheres represent the Li, Fe, oxygen, carbon, and hydrogen atoms, respectively. The FOD structure marked by an asterisk is obtained by considering the geometry of the edge Fe^{2+} ions and their hydroxyl groups and water molecules fixed (rigid).
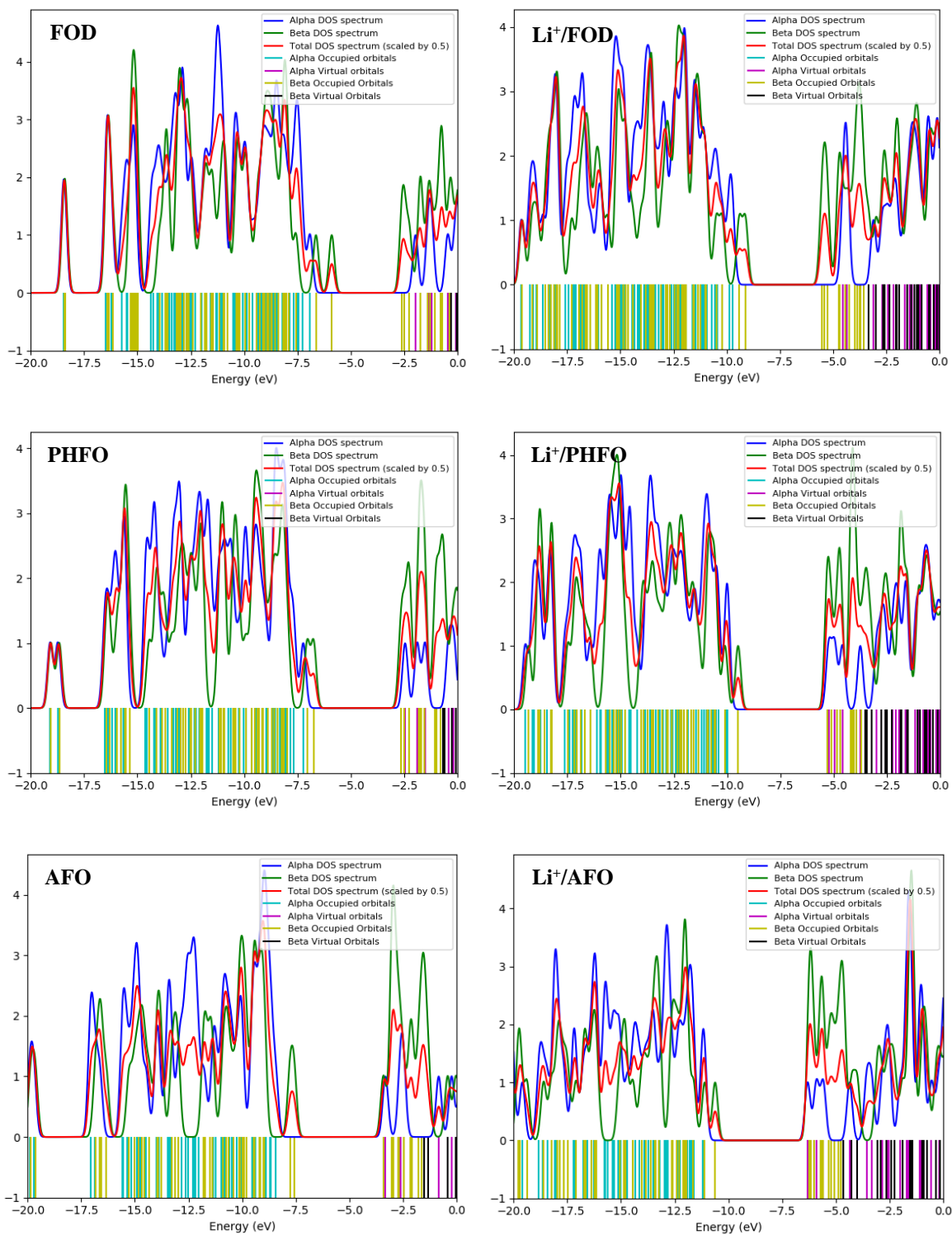
Figure S5. Changes in the density of states (DOS) of FOD, PHFO and AFO upon Li$^+$ intercalation, at the PBE0/cc-pVDZ level.
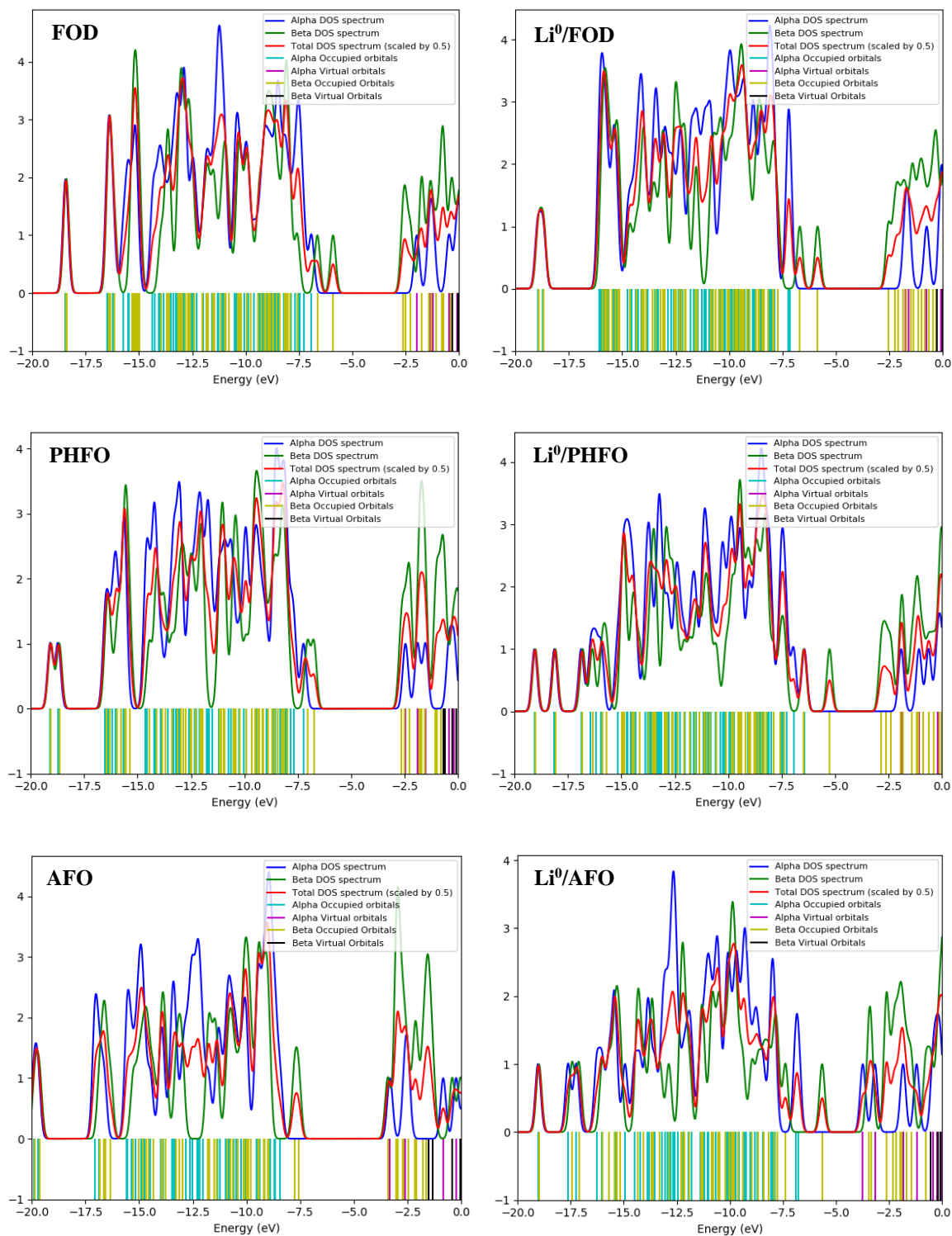
Figure S6. Changes in the density of states (DOS) of FOD, PHFO and AFO upon Li^0 intercalation, at the PBE0/cc-pVDZ level.

References

1. Müller, H.; Bourcet, L.; Hanfland, M. Iron (II) oxalate dihydrate—humboldtine: synthesis, spectroscopic and structural properties of a versatile precursor for high pressure research. *Minerals* **2021**, 11, 113.

2. Echigo, T.; Kimata, M. Single-crystal X-ray diffraction and spectroscopic studies on humboldtine and lindbergite: weak Jahn–Teller effect of Fe^{2+} ion. *Phys. Chem. Miner.* **2008**, 35, 467-475.

3. Li, K.; Liang, Y.; Yang, J.; Yang, G.; Xu, R.; Xie, X. α-Ferrous oxalate dihydrate: an Fe-based one-dimensional metal organic framework with extraordinary photocatalytic and Fenton activities. *Catal. Sci. Technol.* **2018**, 8, 6057-6061.

4. Fan, X.; Zhang, L.; Cheng, R.; Wang, M.; Li, M.; Zhou, Y.; Shi, J. Construction of graphitic C_3N_4-based intramolecular donor–acceptor conjugated copolymers for photocatalytic hydrogen evolution. *ACS Cata.* **2015**, 5, 5008-5015.